INTERACTIONS BETWEEN MACROPARTICLES AND HIGH-ENERGY PROTON BEAMS

S. Rowan*, A. Apollonio, B. Auchmann, A. Lechner, O. Picha, W. Riegler, H. Schindler, R. Schmidt, F. Zimmermann, CERN, Geneva, Switzerland

Abstract

A known threat to the availability of the LHC is the interaction of macroparticles (dust particles) with the LHC proton beam. At the foreseen beam energy of 6.5 TeV during Run 2, quench margins in the superconducting magnets will be 2-3 times less, and beam losses due such interactions may result in magnet quenches. The study introduces an improved numerical model for such interactions, as well as Monte-Carlo simulations that give the probability of such events resulting in a beam-dump during Run 2.

INTRODUCTION

The phenomenon of UFOs (Unidentified Falling Objects), i.e., interactions of falling macroparticles (dust particles) with the proton beam, is well documented [1, 2]. Similar effects are known from other, mostly electron and anti-proton machines [3, 4, 5]. The LHC is the first proton machine where this phenomenon can be found. Figure 1 shows observations of UFO rates during the LHCs Run 1 with beam energies up to 4 TeV. With up to 13 UFOs per hour during a 25-ns bunch-spacing test run, falling macroparticles were estimated to become a significant threat to the availability of the LHC when operating at 6.5 TeV [6]. Such interactions produce particle showers that deposit energy in the adjacent superconducting magnets, possibly leading to magnet quenches. The current strategy to mitigate the effects this phenomenon is to detect the beam-losses with beam-loss monitors, and to trigger a preventative beam dump as soon as a threshold is exceeded.

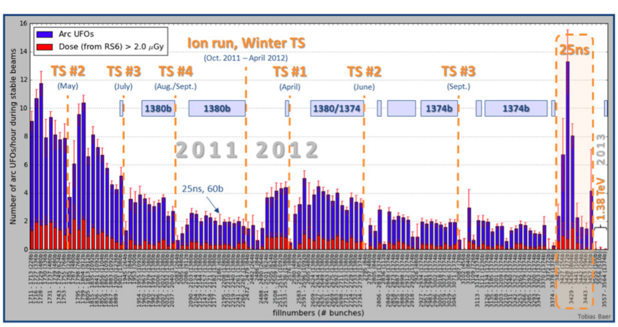

Figure 1: Number of arc UFOs per hour during stable beams in 2011 and 2012. Courtesy T. Baer.

There have been a number of detailed particle-shower simulations and beam-loss experiments to improve the understanding of such quench events [7, 8]. In order to estimate the true extent of the threat and to study relevant mitigation strategies, a numerical model of such macroparticle-to-beam interactions has been constructed, progressing on previous works [9, 10]. The simulated proton-loss rate was translated into signals in the beam-loss monitors (BLMs) based on the above particle-shower simulations. With this model, Monte-Carlo simulations have been carried out to reproduce measured data from 2012, and to extrapolate to Run 2 operating conditions.

NUMERICAL MODEL

A typical interaction between a macroparticle and the high-energy proton beam interaction - commonly referred to as a UFO event, is described as follows:

- A macroparticle (dust) falls from the beam screen or vacuum chamber.
- The macroparticle is ionized by elastic collisions with the proton beam releasing free electrons.
- Inelastic collisions result in particle showers recorded by BLMs, and potential quenches.
- The macroparticle is repelled by the beam's electric field.

Equation of Motion

The macroparticle's acceleration $\ddot{\vec{r}}$, with $\vec{r}$ the transverse position vector, is determined by gravity and by the force exerted by the electric field of the beam $\vec{E}$ on the macroparticle charge Qe,

$$\ddot{\vec{r}}(x, y, t) = \frac{Q(t)e}{m}\vec{E}(x, y) + \vec{g}, \tag{1}$$

with e the electron charge, m the macroparticle mass, g the gravitational constant, and $\vec{E}$ modeled by the Bassetti-Erskine formula [11] with recommendations for numerical stability from [12]. The total beam charge per unit length is given by $N_\mathrm{p}e/C$, with C the LHC circumference and N_p the total number of protons in the beam.

Macroparticle Charge Rate

Elastic interactions with the macroparticle lead to ionization. As a result, the charge rate, $\dot{Q}$, determines the beam's electric field influence. The charging formula, which is related to the Bethe-Bloch formula, is derived from the distribution N_e of knock-on electrons found in [13] with appropriate approximations,

$$\frac{\partial^2 N_\mathrm{e}}{\partial T \partial z} \approx 2\pi r_\mathrm{e}^2 m_\mathrm{e} c_0^2 n \frac{1}{T^2}. \tag{2}$$

* scott.rowan@cern.ch, s.rowan.1@researach.gla.ac.uk, with CERN, Switzerland, and The University of Glasgow, United Kingdom

ISBN 978-3-95450-168-7

where T is the kinetic energy transferred to the electron, z is the incident proton's path length through the material, $r_{\mathrm{e}} = e^2/(4\pi\varepsilon_0 m_{\mathrm{e}} c_0^2)$ is the classical electron radius, with m_{e} the electron mass, ε_0 the vacuum permeability, and c_0 the vacuum speed of light, $n = (N_{\mathrm{A}} Z \rho)/(A M_{\mathrm{u}})$ is the electron density, with N_{A} Avogadro's number, Z and A the atomic number and relative atomic mass of the macroparticle material, respectively, ρ its mass density, and M_{u} the molar mass constant, and m_{e} is the electron mass. In [14, p. 7] we find an empirical fit for the practical range $\ell(T)$ of an electron in a given material as a function of its kinetic energy. This relation can be inverted to give the minimum energy required for a given distance, $T(\ell)$. Assuming that electrons at the minimum escape energy travel perpendicularly to the path of the incident proton, the average path length to escape the macroparticle is $\ell_{\mathrm{esc}} = 0.736R$. The minimum energy-transfer for ionization $T_{\mathrm{min}}(Q(t), R)$ is the sum of $T(\ell_{\mathrm{esc}}(R))$ and the Coulomb potential of the macroparticle at its radius R. The resulting charge-rate formula reads

$$\dot{Q}(x, y, t) = \int_a \int_S \int_{T_{\mathrm{min}}}^{\infty} J(x, y) \frac{\partial^2 N_{\mathrm{e}}}{\partial T \partial z} \,\mathrm{d}T \,\mathrm{d}z \,\mathrm{d}a, \quad (3)$$

where a is the macroparticle's cross-sectional area, S the average path-length of the incident proton through the particle, and J is 2-D Gaussian beam-current density with a total current of $N_{\mathrm{p}} e f$, where f is the LHC revolution frequency. Evaluation, under the assumption that the particle-size is small as compared to the beam size, gives

$$\dot{Q}(x, y, t) = - \frac{2 N_{\mathrm{p}} f R^3 \pi N_{\mathrm{A}} r_{\mathrm{e}}^2 m_{\mathrm{e}} c_0^2 \rho}{3 \sigma_x \sigma_y T_{\mathrm{min}}(Q(t), R) M_{\mathrm{u}}} \mathrm{e}^{-\frac{-x^2}{2\sigma_x^2} - \frac{-y^2}{2\sigma_y^2}}, \quad (4)$$

where $\sigma_{x,y}$ are standard deviations of the 2-D Gaussian beam. The beam size is related to the beta function β (see Fig. 2) and the emittance ϵ via $\sigma_{x,y}(T_{\mathrm{p}}, s) = \sqrt{\beta(s)\epsilon(T_{\mathrm{p}})}$, with T_{p} the proton's kinetic energy. Furthermore, dispersion and momentum offsets are taken into account. From (4), one can derive the average charge per proton, $Q_{\mathrm{pp}} = \dot{Q} / \int_a J \,\mathrm{d}a$, on an uncharged macroparticle, i.e., $T_{\mathrm{min}} = T_{\mathrm{min}}(0, R)$, and compare it to the same value computed with the Garfield++ software [16]. Comparing both

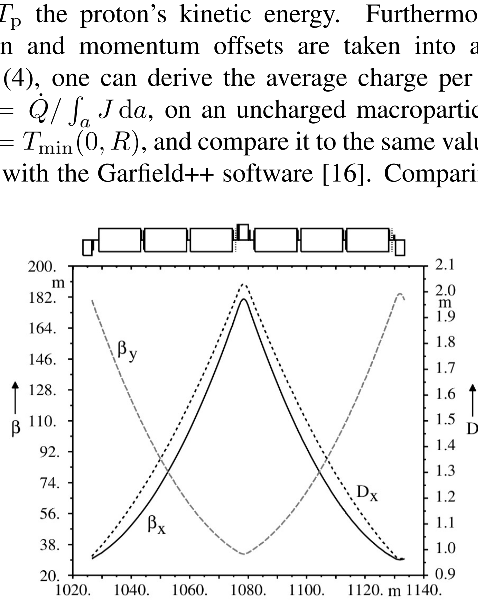

Figure 2: β function and dispersion in an LHC arc cell [15].

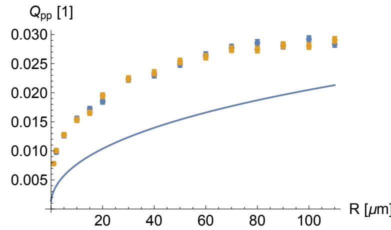

Figure 3: Comparison of the average ionization charges per passing proton by the analytical model and from Garfield++ [16].

shows a good qualitative, and relatively quantitative agreement, see Fig. 3.

Beam Losses

The BLM signal during an interaction is calculated by the product of the BLM response at a given location and the proton loss rate,

$$\mathrm{BLMSignal}(t, s) = \dot{N}_{\mathrm{p}}(\vec{r}(t)) \cdot \mathrm{BLMResponse}(T_{\mathrm{p}}, s), \quad (5)$$

where is s the longitudinal position, $\mathrm{BLMResponse}(T_{\mathrm{p}}, s)$ (see Fig. 4 for a FLUKA [17, 18] simulation) is the BLM signal due to a single inelastic proton-nucleus interaction for a proton of kinetic energy T_{p}. The proton loss rate $\dot{N}_{\mathrm{p}}$ is equal to the rate of inelastic collisions produced by incident protons as they pass through the macroparticle,

$$\dot{N}_{\mathrm{p}}(x, y) = \int_a \int_S J(x, y) \Sigma_{\mathrm{iel}} \,\mathrm{d}s \,\mathrm{d}a, \quad (6)$$

where $\Sigma_{\mathrm{iel}} = \sigma_{\mathrm{iel}} \rho_{\mathrm{A}}$ is the macroscopic cross-section of inelastic interactions, σ_{iel} the microscopic cross-section, and $\rho_{\mathrm{A}} = (N_{\mathrm{A}} \rho)/(A M_{\mathrm{u}})$ the atom density. The resultant formula is thus

$$\dot{N}_{\mathrm{p}}(x, y) = \frac{2 N_{\mathrm{p}} f \sigma_{\mathrm{iel}} R^3 N_{\mathrm{A}} \rho}{3 \sigma_x \sigma_y A M_{\mathrm{u}}} \mathrm{e}^{-\frac{-x^2}{2\sigma_x^2} - \frac{-y^2}{2\sigma_y^2}}. \quad (7)$$

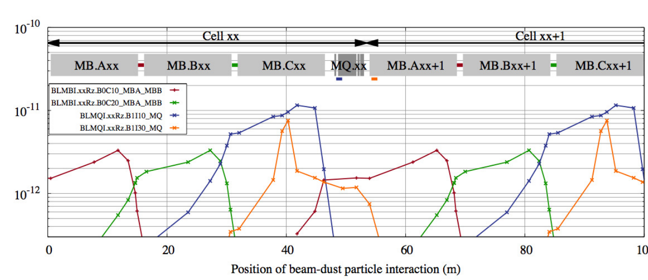

Figure 4: FLUKA-modeled BLM response for the Run-2 configuration, for an inelastic collision of a 6.5-TeV proton with a Carbon nucleus at a given longitudinal location along an arc cell [19].

MONTE-CARLO SIMULATIONS AND 6.5 TeV PREDICTIONS

The numerical model was implemented in Mathematica. Figure 5 shows typical flight paths for different initial transverse locations. Figure 6 demonstrates that the BLM signals of measured UFO events can be reproduced with

ISBN 978-3-95450-168-7

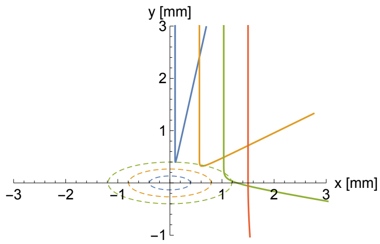

Figure 5: Examples of macroparticle flight-paths for different transverse starting positions. Dashed lines indicate the beam size.

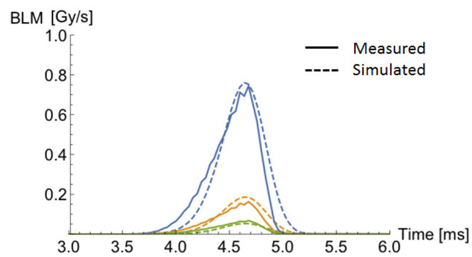

Figure 6: Numerical model (dashed) reproducing the signals of three BLMs (solid) during a UFO event.

realistic input parameters, i.e., a particle of $R = 45\ \mu$m with copper as macroparticle material drops at a plausible location in a standard LHC arc cell. Monte-Carlo simulations were carried out to re-create the recorded UFO events throughout 2012 at 4 TeV beam energy. Figure 7 shows a cumulative histogram of peak BLM signals recorded in three BLM positions, as well as the Monte-Carlo simulated equivalent. The resultant fit required for macroparticle radii distribution, see insert in Fig. 7, using copper as the particle-material (unknown), was, however, produced with physically plausible radii $1 < R < 50\ \mu$m.

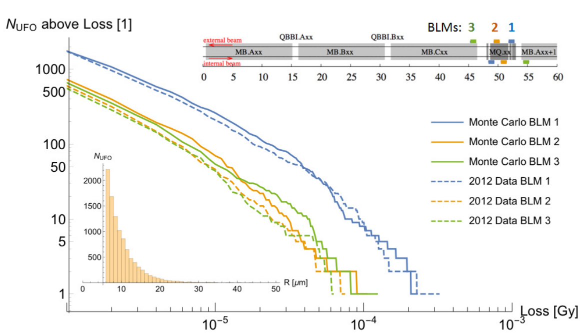

Figure 7: Cumulative histogram of peak BLM signals during UFO events in 2012 (dashed) and Monte-Carlo simulations (solid). Inserts show the radius histogram of the Monte-Carlo and Run-1 BLM positions.

Using the same distributions for location and radii, it was possible to extrapolate to 6.5 TeV by altering beam-related input parameters to the necessary equivalents. Comparing of the upper inserts in Fig. 7 and 8, one can also see the relocation of BLMs for Run 2. This configuration allows for a better sensitivity of the BLM system to UFOs in the dipole magnets.

Throughout Run 2, BLM thresholds will be set at, or just below, the magnet quench limits defined by

$$\mathrm{BLMSignal@Quench}(E, t_{\mathrm{int}}) = \frac{\mathrm{BLMResponse}(E) \cdot \mathrm{QuenchLevel}(E, t_{\mathrm{int}})}{\mathrm{EnergyDeposit}(E)} \quad (8)$$

where t_{int} is the integration time of the BLM signal, EnergyDeposit the average energy deposition in the peak-location of the coil, computed with the same FLUKA model as the BLMResponse, and the QuenchLevel is the minimum energy required to quench. A weakness of the studies predictions, however, is the remaining uncertainty of the QuenchLevel, of a factor of four, quantified in the analysis of dedicated quench tests [20].

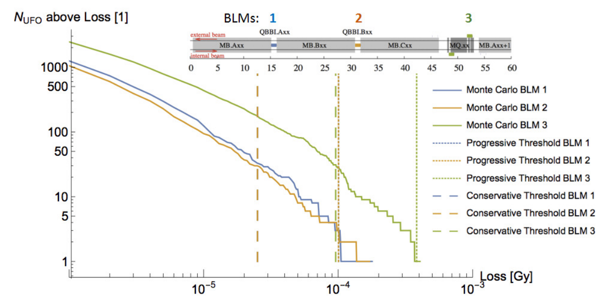

Figure 8: 6.5 TeV Monte-Carlo simulation results including BLM thresholds for conservative and progressive scenarios. Insert shows Run-2 BLM positions.

Figure 8 shows the Monte-Carlo simulation results as well as the Run 2 BLM thresholds for two QuenchLevel scenarios (vertical lines). The QuenchLevel uncertainty has a significant impact on the likelihood of a trip. The predicted percentage of measurable UFO events that lead to a beam dump at 6.5 TeV is 0.11% for the progressive scenario, and 1.24% for the conservative scenario. To obtain absolute numbers, an assumption must be made on the UFO rate. For example, ten UFOs per hour, ten hours of operation per day/seven days a week, would result in one beam dump per week in the progressive scenario, but nine dumps per week in the conservative scenario. Mitigation strategies, such as the blow-up of a number of “defender bunches” to a larger emittance, are being considered and can be successfully modeled.

SUMMARY

The improved model of macroparticle-beam interactions, in combination with a detailed FLUKA simulation of particle showers, allows the generation of a set of UFO events that reproduces 2012 measured data. Adjusting the model parameters allowed for the extrapolation to 6.5 TeV beam energy. Results show that the QuenchLevel uncertainty has a significant impact on the predictions, however, initial Run 2 statistics will be used to negate the uncertainty. To conclude, the model is well suited to simulate such interactions, for making predictions of their influence at higher beam energies and or investigating mitigation strategies.

REFERENCES

[1] T. Baer, M. Barnes, B. Goddard, E. B. Holzer, J. M. Jimenez, A. Lechner, V. Mertens, E. Nebot, A. Nordt, J. Uythoven, B. Velghe, J. Wenninger, and F. Zimmermann. UFOs in the LHC. In *Proceedings of IPAC'11, San Sebastian, Spain*, number TUPC137, 2011.

[2] T. Baer, M. J. Barnes, F. Cerutti, A. Ferrari, N. Fuster, N. Garrel, B. Goddard, E. B. Holzer, S. Jackson, A. Lechner, V. Mertens, M. Misiowiec, E. Nebot, A. Nordt, J. Uythoven, V. Vlachoudis, J. Wenninger, C. Zamantzas, and F. Zimmermann. UFOs in the LHC: Observations, studies, and extrapolations. *Proceedings of IPAC 2012, New Orleans, Louisiana, USA*, (THPPP086):3936–3938, 2012.

[3] F. Zimmermann. Trapped dust in HERA and DORIS. DESY HERA 93-08, DESY, Hamburg, Germany, July 1993.

[4] F. Zimmermann, J. T. Seeman, M. Zolotorev, and W. Stoeffl. Trapped macroparticles in electron storage rings. *IEEE Proceedings of the 1995 Particle Accelerator Conference*, 1995.

[5] D. Sagan. Mass and charge measurement of trapped dust in the CESR storage ring. *NIM Section A*, 339:371–379, 1993.

[6] T. Baer, M. J. Barnes, E. Carlier, F. Cerutti, B. Dehning, L. Ducimetiere, A. Ferrari, N. Garrel, A. Gerardin, B. Goddard, E. B. Holzer, S. Jackson, J. M. Jimenez, V. Kain, A. Lechner, V. Mertens, M. Misiowiec, R. Ballester, E. Nebot, L. Drosdal, A. Nordt, J. Uythoven, B. Belghe, V. Vlachoudis, J. Wenninger, C. Zamantzas, F. Zimmermann, and N. Fuster. UFOs in the LHC after LS1. *Proceedings of the 2012 LHC Performance Workshop*, January 2012.

[7] M. Sapinski, B. Auchmann, T. Baer, W. Bartmann, M. Bednarek, S. Bozyigit, C. Bracco, R. Bruce, F. Cerutti, V. Chetvertkova, K. Dahlerup-Petersen, B. Dehning, E. Nebot, E. Effinger, J. Emery, A. Guerrero, W. Hofle, E. B. Holzer, A. Lechner, A. Priebe, S. Redaelli, B. Salvachua, R. Schmidt, N. V. Shetty, A. Siemko, E. Skordis, M. Solfaroli, J. Steckert, J. Uythoven, D. Valuch, A. Verweij, J. Wenninger, D. Wollmann, and M. Zerlauth. Beam-induced quench tests of LHC magnets. *Proceedings of IPAC 2014, Dresden Germany*, (MOOCB01):52–54, 2014.

[8] A. Lechner, et al. Particle Shower Simulations for LHC Quench Tests: Methodology, Challenges and Selected Results. *Proceedings of the Workshop on Beam-Induced Quenches, CERN, Geneva, Switzerland*, 2014.

[9] F. Zimmermann, M. Giovannozzi, and A. Xagkoni. Interaction of macro-particles with LHC proton beam. *Proceedings of IPAC 2010, Kyoto, Japan*, (MOPEC016):492–494, 2010.

[10] N. Fuster Martinez, U. Valencia, F. Zimmermann, T. Baer, M. Giovannozzi, E. B. Holzer, E. Nebot, A. Nordt, M. Sapinski, and Z. Yang. Simulation studies of macroparticles falling into the LHC proton beam. *Proceedings of IPAC 2011, San Sebastian, Spain*, (MOPS017):634–636, 2011.

[11] M. Bassetti and G. A. Erskine. "Closed expression for the electrical field of a two-dimensional gaussian charge". *Technical Note CERN-ISR-TH/80-06, CERN, Geneva, Switzerland, March, 1980.*

[12] V. Ziemann. Beyond Bassetti and Erskine: Beam-beam deflections for non-Gaussian beams. Project Note SLAC-PUB-5582, SLAC, Stanford CA 94309, June 1991.

[13] Particle Data Group. "Review of particle properties". *Phys. Rev. D, 45, 1992.*

[14] W. Blum, W. Riegler, and L. Rolandi. "Particle Detection with Drift Chambers". *Springer, 2nd edition, 2008.*

[15] S. Russenschuck. *Electromagnetic Design and Mathematical Optimization Methods in Magnet Technology*. eBook at http://cern.ch/russ, 3rd edition, February 2006.

[16] H. Schindler, Garfield++ User Guide (Version 2014.1), http://cern.ch/garfieldpp, 2014.

[17] A. Fasso, et al., "FLUKA: a Multi-Particle Transport Code", CERN-2005-10, INFN/TC_05/11, SLAC-R-773, 2005.

[18] G. Battistoni, et al., "The FLUKA Code: Description and Benchmarking", Proceedings of the Hadronic Shower Simulation Workshop 2006 at Fermilab, Batavia, IL, USA, AIP Conference Proceeding, Vol. 896, p. 31–49, 2007.

[19] A. Lechner, B. Auchmann, T. Baer, F. Cerutti, V. Chetvertkova, B. Dehning, E. B. Holzer, O. Picha, M. Sapinski, N. V. Shetty, and E. Skordis. "BLM thresholds for post-LS 1 LHC operation: UFOs and orbit bumps in the arcs and straight sections". submitted to *Proceedings of the Beam-Induced Quenches Workshop, CERN, September 2014.*

[20] B. Auchmann, T. Baer, R. Bruce, F. Cerutti, B. Dehning, L. Esposito, E.B. Holzer, A. Lechner, O. Picha, S. Redaelli, M. Sapinski, N. Shetty, E. Skordis. "BLM Thresholds Strategy (Vis-a-Vis UFOs and Quenches)". *Proceedings of Chamonix 2014 - LHC Perfomance Workshop, Chamonix, France, September 2014 (in press).*

ISBN 978-3-95450-168-7